Structural and Functional Lung Impairment in Primary Ciliary Dyskinesia. Assessment with Magnetic Resonance Imaging and Multiple Breath Washout in Comparison to Spirometry

Nyilas, Sylvia ; Bauman, Grzegorz ; Pusterla, Orso ; Sommer, Gregor ; Singer, Florian ; Stranzinger, Enno ; Heyer, Christoph ; Ramsey, Kathryn ; Schlegtendal, Anne ; Benzrath, Stefanie ; Casaulta, Carmen ; Goutaki, Myrofora ; Kuehni, Claudia E ; Bieri, Oliver ; Koerner-Rettberg, Cordula ; Latzin, Philipp

Abstract: RATIONALE Primary ciliary dyskinesia (PCD) is an inherited disorder characterized by heterogeneous airway disease. Traditional lung function techniques (e.g. spirometry) may underestimate severity and complexity of PCD. OBJECTIVES We assessed lung impairment in individuals with PCD using structural and functional magnetic resonance imaging (MRI) and different lung function techniques. METHODS Thirty study participants with PCD (median 13.4 years, range 5-28) underwent structural and functional MRI, spirometry, and multiple breath washout (MBW) on the same day. Primary endpoints included structural MRI morphology scores, relative ventilation and perfusion impairment from functional MRI, FEV1 from spirometry, and lung clearance index (LCI) from MBW. RESULTS Severity and complexity of PCD lung disease varied significantly between individuals. Structural lung disease was detected in all subjects with a median (IQR) extent score of 10.3 (7 to 19; maximum score = 60). Functional MRI ventilation impairment was present in 52% of subjects affecting 24.2% (21.1 to 25.2%) of the lung. Relative perfusion impairment was detected in 78% of individuals affecting 21.1% (19.4 to 25.9%) of the lung. LCI was abnormal in 83% (median 8.3 (2.6 to 13.2) z-scores) and FEV1 was abnormal in 27% (-0.5 (-1.6 to 0.3) z-scores) of individuals. Concordance between spirometry and imaging outcomes was poor, with 52% of patients showing both abnormal MRI and LCI values, but normal FEV1. CONCLUSIONS Discordance between lung function and imaging outcomes in patients with PCD supports the use of both imaging and lung function, such as MBW, for surveillance of this heterogeneous disease.

DOI: https://doi.org/10.1513/AnnalsATS.201712-967OC

Other titles: Structural and Functional Lung Impairment in PCD: Assessment with MRI and Multiple Breath Washout in Comparison to Spirometry

Myrofora; Kuehni, Claudia E; Bieri, Oliver; Koerner-Rettberg, Cordula; Latzin, Philipp (2018). Structural and Functional Lung Impairment in Primary Ciliary Dyskinesia. Assessment with Magnetic Resonance Imaging and Multiple Breath Washout in Comparison to Spirometry. Annals of the American Thoracic Society, 15(12):1434-1442.
DOI: https://doi.org/10.1513/AnnalsATS.201712-967OC

ANNALSATS Articles in Press. Published on 05-October-2018 as 10.1513/AnnalsATS.201712-967OC

Structural and Functional Lung Impairment in PCD: Assessment with MRI and Multiple Breath Washout in Comparison to Spirometry

Sylvia Nyilas*[1,2,3]; Grzegorz Bauman*[4,5]; Orso Pusterla[4,5]; Gregor Sommer[6]; Florian Singer[1]; Enno Stranzinger[2]; Christoph Heyer[7]; Kathryn Ramsey[1]; Anne Schlegtendal[8]; Stefanie Benzrath[8]; Carmen Casaulta[1]; Myrofora Goutaki[9]; Claudia E. Kuehni[9]; Oliver Bieri[4,5]; Cordula Koerner-Rettberg#[8]; Philipp Latzin#[1]

[1]Pediatric Respiratory Medicine, Department of Pediatrics, Inselspital, Bern University Hospital, University of Bern, Switzerland; [2]Department of Diagnostic, Interventional and Pediatric Radiology Inselspital, University of Bern, Bern, Switzerland; [3]University Children's Hospital Basel (UKBB), Basel, Switzerland; [4]Department of Radiology, Division of Radiological Physics, University of Basel Hospital, Basel, Switzerland; [5]Department of Biomedical Engineering, University of Basel, Basel, Switzerland; [6]Clinic of Radiology and Nuclear Medicine, University Hospital Basel, University of Basel, Switzerland; [7]Institute of Pediatric Radiology, University Children's Hospital, Ruhr-University of Bochum, Germany; [8]Department of Pediatric Pneumology, University Children's Hospital of Ruhr University Bochum at St Josef-Hospital, Bochum, Germany; [9]Institute for Social and Preventive Medicine, University Bern, Bern, Switzerland.

*Contributed equally as first authors.

#Contributed equally as senior authors.

Corresponding Author:
Philipp Latzin, MD, PhD
University Children's Hospital of Bern
Freiburgstrasse 8, 3010 Bern, Switzerland
E-mail: philipp.latzin@insel.ch
Phone: +41 31 632 95 81

Authors' Contributions: SN, GB, OB, CKR and PL designed the study concept. SN, GB, OP, AS, SB, CKR and CH collected study data. SN, GB, OP, ES and GS analyzed the data. SN, GB, GS, FS, ES, OB, KR, MG, CK, CKR and PL interpreted the data. SN and GB drafted the manuscript. All authors revised the manuscript.

Sources of Support: The work for this report was funded by the Swiss National Foundation (Grant number: SNF 320030_149576) and the Botnar Foundation. The researchers are supported by the network of COST Action BEAT-PCD: Short Term Scientific Mission STSM-BM1407. The funding sources had no role in the study design, data collection and analysis, decision to publish, or preparation of the manuscript.

Disclosures: Dr. Latzin reports personal fees from Gilead, Novartis, Polyphor, Roche, Schwabe, Vertex, Vifor and Zambon. Otherwise, no conflicts of interest, financial or otherwise, are declared by the author(s).

Word Count: 2995

Short Running Head: In PCD, MRI provides complementary information

Descriptor Number: 14.6; 14.4

Keywords: Magnetic resonance imaging, lung function, nitrogen multiple breath washout, primary ciliary dyskinesia

This article has a data supplement, which is accessible from this issue's table of contents online at www.atsjournals.org

University of Bern, Switzerland; [2]Department of Diagnostic, Interventional and Pediatric Radiology Inselspital, University of Bern, Bern, Switzerland; [3]University Children's Hospital Basel (UKBB), Basel, Switzerland; [4]Department of Radiology, Division of Radiological Physics, University of Basel Hospital, Basel, Switzerland; [5]Department of Biomedical Engineering, University of Basel, Basel, Switzerland; [6]Clinic of Radiology and Nuclear Medicine, University Hospital Basel, University of Basel, Switzerland; [7]Institute of Pediatric Radiology, University Children's Hospital, Ruhr-University of Bochum, Germany; [8]Department of Pediatric Pneumology, University Children's Hospital of Ruhr University Bochum at St Josef-Hospital, Bochum, Germany; [9]Institute for Social and Preventive Medicine, University Bern, Bern, Switzerland.

[*] Contributed equally as first authors.

[#] Contributed equally as senior authors.

Corresponding Author:
Philipp Latzin, MD, PhD
University Children's Hospital of Bern
Freiburgstrasse 8, 3010 Bern, Switzerland
E-mail: philipp.latzin@insel.ch
Phone: +41 31 632 95 81

Authors' Contributions: SN, GB, OB, CKR and PL designed the study concept. SN, GB, OP, AS, SB, CKR and CH collected study data. SN, GB, OP, ES and GS analyzed the data. SN, GB, GS, FS, ES, OB, KR, MG, CK, CKR and PL interpreted the data. SN and GB drafted the manuscript. All authors revised the manuscript.

Sources of Support: The work for this report was funded by the Swiss National Foundation (Grant number: SNF 320030_149576) and the Botnar Foundation. The researchers are supported by the network of COST Action BEAT-PCD: Short Term Scientific Mission STSM-BM1407. The funding sources had no role in the study design, data collection and analysis, decision to publish, or preparation of the manuscript.

Disclosures: Dr. Latzin reports personal fees from Gilead, Novartis, Polyphor, Roche, Schwabe, Vertex, Vifor and Zambon. Otherwise, no conflicts of interest, financial or otherwise, are declared by the author(s).

Word Count: 2995

ANNALSATS Articles in Press. Published on 05-October-2018 as 10.1513/AnnalsATS.201712-967OC

Abstract

Rationale: Primary ciliary dyskinesia (PCD) is an inherited disorder characterized by heterogeneous airway disease. Traditional lung function techniques (e.g. spirometry) may underestimate severity and complexity of PCD.

Objectives: We assessed lung impairment in individuals with PCD using structural and functional magnetic resonance imaging (MRI) and different lung function techniques.

Methods: Thirty study participants with PCD (median 13.4 years, range 5–28) underwent structural and functional MRI, spirometry, and multiple breath washout (MBW) on the same day. Primary endpoints included structural MRI morphology scores, relative ventilation and perfusion impairment from functional MRI, FEV_1 from spirometry, and lung clearance index (LCI) from MBW.

Results: Severity and complexity of PCD lung disease varied significantly between individuals. Structural lung disease was detected in all subjects with a median (IQR) extent score of 10.3 (7 to 19; maximum score = 60). Functional MRI ventilation impairment was present in 52% of subjects affecting 24.2% (21.1 to 25.2%) of the lung. Relative perfusion impairment was detected in 78% of individuals affecting 21.1% (19.4 to 25.9%) of the lung. LCI was abnormal in 83% (median 8.3 (2.6 to 13.2) z-scores) and FEV_1 was abnormal in 27% (-0.5 (-1.6 to 0.3) z-scores) of individuals. Concordance between spirometry and imaging outcomes was poor, with 52% of patients showing both abnormal MRI and LCI values, but normal FEV_1.

Conclusions: Discordance between lung function and imaging outcomes in patients with PCD supports the use of both imaging and lung function, such as MBW, for surveillance of this heterogeneous disease.

Primary ciliary dyskinesia (PCD) is an autosomal recessive inherited disorder of considerable clinical and genetic heterogeneity (1). The main feature of PCD is decreased airway clearance due to impaired ciliary motility (2). This results in localized airway infections, ventilation defects, and heterogeneous impairments to pulmonary function and structure (1, 3-5). A major challenge of the current clinical care in PCD is the ability to detect and monitor subclinical lung disease (5, 6). Spirometry has been traditionally used to assess airflow limitation (7-9), while the multiple breath washout (MBW) technique is more sensitive to detect subclinical small airway disease (10). Still, lung function tests alone cannot differentiate between reversible and irreversible structural defects and may underestimate disease severity.

Lung imaging is thus needed to directly assess the presence and extent of structural lung disease in individuals with PCD. High-resolution computed tomography (HR-CT) is considered the gold standard for assessing structural abnormalities in lung disease (7, 11, 12). However, HR-CT scans expose individuals to ionizing radiation and functional information from HR-CT scans is limited (13, 14). Beside HR-CT, Magnetic resonance imaging (MRI) techniques can provide information on structural and functional deficits in the lung without radiation exposure (15). Traditionally functional MRI techniques were constrained by the need for intravenous or inhaled contrast agents (16-20). However, recently developed matrix pencil (MP) decomposition MRI method can be used to assess ventilation and perfusion defects in the lung during free tidal breathing and without the need for contrast agents (21). We have previously shown that the functional MP-MRI method is sensitive to detect lung ventilation and perfusion impairment in children with cystic fibrosis (CF), and there is a high degree of correlation between lung structure and function outcomes in this population (15). We hypothesized that

ANNALSATS Articles in Press. Published on 05-October-2018 as 10.1513/AnnalsATS.201712-967OC

functional MP-MRI will also detect impairment of ventilation and perfusion in individuals with PCD. Specifically we aimed to assess (i) the prevalence and extent of lung function and structure abnormalities, and (ii) the concordance and correlation between lung function and structural outcomes in individuals with PCD. Some of the data have been presented previously in abstract form (22).

Methods

Study Design

This is a prospective cross-sectional, single-centre observational study. Recruitment took place between April 2015 and February 2016. Study participants underwent spirometry, nitrogen multiple breath washout (N_2-MBW), structural MRI, and functional MP-MRI on the same day.

Study Population

We enrolled 30 study participants with PCD, aged 5–28 years (median age 13.4 years) at the University Children`s Hospital of Ruhr University Bochum, St Josef Hospital, Germany. All study participants had a confirmed diagnosis of PCD according to current guidelines and clinical symptoms coherent to PCD diagnosis (5, 23, 24) (Table 1, E1). Eligibility criteria included the absence of acute pulmonary exacerbation during the last three weeks prior to the study (25). The study was approved by the Ethics Committee of the Ruhr University Bochum (Number: 5103). We obtained written informed consent from parents and assent from study participants if older than 14 years.

MRI Data Acquisition and Evaluation

All MRI examinations were performed on a 1.5 Tesla whole-body MR-scanner (MAGNETOM Avanto-Fit, Siemens Healthineers, Erlangen, Germany) using a 12-channel thorax and a 24-channel spine receiver coil array. Both structural and functional MRI were obtained during free breathing and without the use of contrast agents within a single MR session. Sedation was not required for MRI assessment, even for the youngest patient (aged 5 years).

Morphological MRI

The *Eichinger* MRI morphology score was used to assess the presence and extent of structural lung disease (26). The structural defects assessed include bronchiectasis/bronchial wall thickening, mucus plugging, abscess/sacculation, special findings and consolidation. Individual features are scored as follows: 0 = not present; 1 = present and affecting ≤ 50% of the lobe; 2 = present and affecting > 50% of the lobe. The lobe scores for each component were summed to produce a score out of 12. The total morphology score is composed of five sub-scores each with a maximum score of 12 (maximum score = 60). The morphological MRI datasets were scored by two board-certified, fellowship-trained radiologists with 9 and 14 years of experience in cross-sectional imaging of the chest. Further details are provided in the online supplement (Table E2).

Functional MRI

Functional MRI imaging was performed using the recently developed matrix pencil decomposition method (MP-MRI), which is a derivative of the Fourier decomposition MRI technique (27-30). Functional MRI imaging was performed using time-resolved acquisitions

ANNALSATS Articles in Press. Published on 05-October-2018 as 10.1513/AnnalsATS.201712-967OC

with an ultra-fast steady-state free precession (ufSSFP) pulse sequence during relaxed breathing. The matrix pencil decomposition method was applied to generate maps of regional fractional ventilation, which reflects changes of lung parenchyma density during respiration, and regional perfusion maps, which reflects changes in blood flow in the lung (21, 30). The distribution of ventilation and perfusion was assessed and a threshold was applied to determine the degree of impairment (15, 29). The relative fractional ventilation (R_{FV}) and relative perfusion (R_Q) impairment were calculated and expressed as a percentage of lung volume for each study participant. In order to estimate the degree of functional abnormalities in patients with PCD we relied on historical normal values for MRI (15).
Further details are provided in the online supplement.

Lung Function Assessment

Spirometry. Spirometry was performed using Jaeger MasterScreen bodyplethysmograph equipment (CareFusion, Hochberg, Germany) according to current guidelines (8). We assessed the forced expiratory volume in 1 second (FEV_1) and forced vital capacity (FVC) and calculated z-scores from recommended reference equations for spirometry (31).

Multiple breath washout (MBW). The nitrogen multiple breath washout (N_2-MBW) technique was performed using a commercially available device (Exhalyzer D, Eco Medics AG, Duernten, Switzerland) (32) and in accordance with current consensus guidelines (33, 34). The primary outcome was the lung clearance index (LCI). Secondary outcomes included S_{cond} and S_{acin}, which reflect convection and diffusion-convection dependent ventilation inhomogeneity, respectively. We calculated z-scores for the N_2-MBW based on published reference values (9).

Statistical Analysis

Visual inspection of the distribution of our data indicated significant skewing, therefore the data were expressed as medians and interquartile ranges (IQRs). To assess the prevalence and concordance of structural and functional outcomes we defined abnormality at ±1.64 z-scores for spirometry and MBW outcomes(35), structural MRI sub-scores ≥ 2 points (indicates >15% structural impairment) (36), and functional MRI outcomes $R_{FV} \geq 24.2\%$ and $R_{Q} \geq 19.3\%$ according to healthy reference data (15). We described concordance for the entire population using a Venn diagram and further in four study participants to illustrate clinical phenotypes. Spearman`s rank correlation coefficients (r) were used to assess correlations between structural and functional outcomes (correlations definitions: weak (0.10-0.29), moderate (0.30-0.49) and strong (>0.50)) (37). We used the mean morphological scores from both readers to assess the extent of structural lung disease. Inter-observer agreement was calculated using the intra class correlation coefficient (ICC). P-values <0.05 were considered statistically significant. Analyses were performed using Stata (Stata Statistical Software: Release 13. College Station, TX: StataCorp LP). Graphs were drawn with Stata and MATLAB (2012b, The MathWorks, Natick, MA, US). Additional details are provided in the online supplement.

Results

All thirty subjects with PCD were able to perform spirometry, N_2-MBW, and MRI on the same day. The clinical characteristics of the study participants are presented in Table 1 and Table E1.

ANNALSATS Articles in Press. Published on 05-October-2018 as 10.1513/AnnalsATS.201712-967OC

Data Quality

After quality control, all 30 study participants had morphological MRI, N_2-MBW and spirometry data, and 27 study participants had functional MRI data, included in the final analysis. Further details are provided in the online supplement.

Magnetic Resonance Imaging

Structural lung abnormalities were present in all study participants. The proportion of study participants with bronchiectasis/ bronchial wall thickening was 97% and mucus plugging was 60% (Table 2). The total morphology score ranged from 3 to 28 and the median (IQR) score for the population was 10.3 (7 to 19). The bronchiectasis/bronchial wall thickening scores ranged from 1.5 to 10.5 and the median (IQR) score was 6 (4.5 to 8). The mucus plugging score ranged from 0.5 to 8.5 and the median (IQR) score was 2.3 (1 to 4). We found a predominance of defects in the middle and lower lobes (Table E3). The agreement between structural MRI readers was good with an ICC of 0.67 for the total morphology score (Table E2).

The proportion of study participants with functional MRI ventilation impairment was 52% and perfusion impairment was 78%. The relative proportion of the lung with impaired ventilation (R_{FV}) (median (IQR)) was 24.2% (21.1 to 25.2) and relative perfusion (R_Q) was, 21.1% (19.4 to 25.9) (Table 2).

Lung Function

The ability to capture abnormal lung function strongly varied between techniques. The proportion of subjects with abnormal values was 27% for FEV_1, 83% for LCI, 63% for S_{cond}, and

50% for S_{acin}. The median (IQR) of FEV_1 z-score was -0.5 (-1.6 to 0.3), LCI was 8.3 (2.6 to 13.2) z-score, S_{cond} 2.8 (0.9 to 4.4) z-score, and S_{acin} 1.7 (0.4 to 6.7) z-score (Table 3).

Concordance between Lung Function and MRI on Group and Individual Level

More than half of the patients (52%) had structural lung disease, functional MRI impairment and abnormal LCI values, but FEV_1 values within the normal range (Figure 1). Only 15% of subjects had concordant abnormalities in all primary outcome measures. In terms of concordance between two primary outcomes, LCI and total morphology score were concordantly abnormal in 25 of 30 (83%) subjects, mucus plugging and LCI were concordantly abnormal in 15/30 (50%) subjects, and LCI and R_Q were concordantly abnormal in 19/27 (70%) subjects.

To illustrate the complexity of PCD lung disease, MRI and lung function from four individual study participants are presented in Table E4. Subjects 1 and 2 had FEV_1 values within the normal limits, while subjects 3 and 4 had abnormal FEV_1. In contrast, subjects 1 and 4 had normal LCI values, while subjects 2 and 3 had pathological LCI values, which differed in severity of 7.3 and 24.0 z-scores, respectively. Morphological MRI scores also differed between these subjects. Patient 2 is a 28 year-old female (morphology score = 5) who had rarefaction of the lung parenchyma in the upper lobes, resembling emphysematous changes (a finding that is not captured by score). Patient 3 showed more extensive bronchiectasis/ bronchial wall thickening without atelectasis (score = 26). Both these subjects had poorly perfused and ventilated lung regions, although functional impairment on MRI was more pronounced in Patient 3. The results from these study participants are outlined in Table E4, Figure 1 and Figure 2.

ANNALSATS Articles in Press. Published on 05-October-2018 as 10.1513/AnnalsATS.201712-967OC

Correlation between Structure and Function Outcomes

Lung function and functional MRI outcomes cannot distinguish between reversible (mucus plugging) and partly irreversible (bronchiectasis/bronchial wall thickening) structural changes (Figure 3, Figure E1 and E2). There were no statistically significant correlations between functional MRI and lung function outcomes (Figure 4 and Table E5). However, we found statistically significant, moderate correlations between the total morphology scores and LCI ($r = 0.54$, $p = 0.002$) and FEV_1 ($r = -0.59$, $p < 0.001$) (Table E5, Figure E3).

Discussion

We used comprehensive imaging and function methods to assess lung disease in individuals with PCD. PCD lung disease is characterized by highly prevalent structural pathology with heterogeneous functional consequences. Structural lung disease, functional MRI impairment, and abnormal LCI were present in the majority of patients. FEV_1, however, was not sensitive enough to detect structural airway disease in this population. Our findings highlight the heterogeneous nature of PCD lung disease and the need for a multi-modality approach to characterize and potentially monitor patients with PCD.

Comparison with Previous Literature

We assessed structural lung abnormalities in patients with PCD using morphological MRI. Previous studies have only used HR-CT imaging to characterize structural lung disease in patients with PCD (7, 11). However, studies have shown that MRI can reliably assess structural

lung disease in patients with CF lung disease (18, 38) and demonstrated good agreement between HR-CT and MRI in patients with PCD (39). We found that the prevalence and extent of structural lung abnormalities in patients with PCD was similar to what we reported in patients with CF (15). Therefore, our results indicate that morphological MRI scans can provide a radiation-free method to assess structural lung disease in individuals with PCD.

We found that the correlation between lung structure and function outcomes were weaker in patients with PCD compared with those we reported in patients with CF. Structural lung abnormalities e.g. bronchiectasis/bronchial wall thickening were present in 97% of all subjects, while 78% of subjects had abnormal LCI and only 27% had abnormal FEV_1. Previous studies using HR-CT have reported a strong correlation between LCI and CT morphology scores ($r = 0.8$) (7), while another reported no correlation (11). The conflicting nature of these data also suggest a multi-modality approach to fully and reliably characterize PCD lung disease.

The major advantage of the functional MRI technique used in our study is that it provides data on ventilation and perfusion impairment in the lung without the need for contrast agents or breath-hold manoeuvres (18, 20). This is the first time this technique has been used to assess functional lung impairment in patients with PCD. In contrast to patients with CF, we did not find a correlation between perfusion and ventilation indices from the functional MRI and lung function outcomes in patients with PCD (15). A previous study used hyperpolarised gas MRI to assess lung ventilation defects in patients with PCD and reported good correlations between imaging and lung function outcomes (LCI and FEV_1/FVC) (20). Lung impairment in patients with PCD is frequently focal in nature with lobar or segmental atelectasis. Focal pathology is difficult to capture by lung function techniques that assess global

ANNALSATS Articles in Press. Published on 05-October-2018 as 10.1513/AnnalsATS.201712-967OC

airflow or ventilation impairment. We determined in our analysis that middle and lower lobe were more severely (score = 2) and more predominant affected than the upper lobe. This is in line with previously studies which showed typical imaging features in PCD including a predominance of bronchiectasis in the middle and lower lobes (40, 41) presumably due to greater difficulty in the drainage of secretions. Therefore, relationships between lung imaging and function outcomes can be influenced by the heterogeneity of the disease in individuals with PCD (42). Further work to define morphological and functional scoring systems specific for the focal nature of lung disease in individuals with PCD is needed.

Clinical Relevance

We recruited individuals with PCD diagnosed based on current European consensus recommendations (5, 23, 24). Our patient population included a wide age range, with a variety of disease severities, and therefore represents a typical PCD population in tertiary care centres. We provide further evidence that FEV_1 is not sensitive to monitor structural airway pathologies in patients with PCD. The LCI from the MBW technique appears to be more sensitive to monitor early structural lung disease, however, LCI values were not able to distinguish between individuals with reversible and partly irreversible structural disease. Therefore, in patients with normal lung function, lung imaging may be needed to detect early and focal structural changes. Structural and functional MRI are sensitive tools to monitor lung disease progression and responses to treatment without the need for radiation exposure or the risks associated with intravenous contrast agents.

Strengths and Limitations

All study participants enrolled in our study were able to perform MRI scans and lung function tests within a one-day clinic visit. All MR images were obtained without sedation, contrast agent or breathing maneuvers which can be difficult in younger or uncooperative subjects. We included thirty study participants with clear and fulfilled PCD diagnostic criteria. The sample size is comparable to previous studies and is sufficient to allow meaningful interpretation of the data (7, 11, 15). The patients with PCD in our study were younger (mean 13.4 (range 10.4 to 17.1), than the patients in the study of Boon (16.1 (11.1 to 19.6) years) and Irving (mean age of 24.7), and therefore have a milder lung disease compared with the older patients in these studies. We did not include retrospective chest CT scans as this data was not available within a reasonable time before the MRI scans to allow meaningful comparison. We used an established MRI CF score to evaluate structural disease in study participants with PCD (26). The ICC between scorers was good in our study. However, PCD specific CT and MRI morphology scorings systems are currently not available. Peripheral bronchiectasis without bronchial wall thickening, and discrete mucus plugging of small airways cannot be well visualized by MRI (14). In addition, hyperinflation of the lung may be underestimated using a CF scoring system. We did not recruit prospective healthy controls in this study but relied on previously published normative data from our group using the same equipment for both MRI and lung function outcomes (15). Furthermore, the automatic functional lung evaluation method as used in this work relies on segmentation of the whole lung volume in order to calculate global ventilation or perfusion impairment. Currently, no lobar segmentation method is available as it poses a significant

ANNALSATS Articles in Press. Published on 05-October-2018 as 10.1513/AnnalsATS.201712-967OC

challenge in comparison to well-established lobar segmentation methods known from computed tomography.

Outlook

Sensitive and feasible techniques for functional lung MRI in children are now available. We encourage the use of MRI for future investigative studies in patients with PCD to allow for better understanding of this complex lung disease. Future interventional trials should consider the use of a combination of novel MRI techniques and lung function outcomes to collectively monitor responses to treatments in PCD lung disease.

Conclusion

In summary, we assessed airflow limitation, ventilation, perfusion, and structural airway impairment in patients with PCD using novel MRI sequences without the need for contrast agents or breathing manoeuvres. The poor correlation between spirometry and imaging outcomes in our study supports the use of both MRI and sensitive lung function techniques to assess lung disease in individuals with PCD. While LCI was more sensitive to detect lung disease than FEV_1, LCI was not able to discriminate between reversible and irreversible airway disease in our study. Longitudinal studies using a combination of MRI and LCI may help to understand the complex relationships between PCD genotypes, ciliary function phenotypes, lung morphology and functional impairment.

Acknowledgements

The authors would like to thank all of the children and their families for their participation in the study. The authors would like to express their gratitude to all the study nurses for their patient care and support with measurements, as well as Sharon Krattinger, Sandra Lüscher and Romy Rodriguez for their help in measurement analysis.

ANNALSATS Articles in Press. Published on 05-October-2018 as 10.1513/AnnalsATS.201712-967OC

References

1. Davis SD, Ferkol TW, Rosenfeld M, Lee HS, Dell SD, Sagel SD, Milla C, Zariwala MA, Pittman JE, Shapiro AJ, Carson JL, Krischer JP, Hazucha MJ, Cooper ML, Knowles MR, Leigh MW. Clinical features of childhood primary ciliary dyskinesia by genotype and ultrastructural phenotype. Am J Respir Crit Care Med 2015; 191: 316-324.
2. Afzelius BA. A human syndrome caused by immotile cilia. Science 1976; 193: 317-319.
3. Noone PG, Leigh MW, Sannuti A, Minnix SL, Carson JL, Hazucha M, Zariwala MA, Knowles MR. Primary ciliary dyskinesia: diagnostic and phenotypic features. Am J Respir Crit Care Med 2004; 169: 459-467.
4. Adam D, Roux-Delrieu J, Luczka E, Bonnomet A, Lesage J, Merol JC, Polette M, Abely M, Coraux C. Cystic fibrosis airway epithelium remodelling: involvement of inflammation. J Pathol 2015; 235: 408-419.
5. Barbato A, Frischer T, Kuehni CE, Snijders D, Azevedo I, Baktai G, Bartoloni L, Eber E, Escribano A, Haarman E, Hesselmar B, Hogg C, Jorissen M, Lucas J, Nielsen KG, O'Callaghan C, Omran H, Pohunek P, Strippoli MP, Bush A. Primary ciliary dyskinesia: a consensus statement on diagnostic and treatment approaches in children. Eur Respir J 2009; 34: 1264-1276.
6. Maglione M, Montella S, Santamaria F. Chest CTs in primary ciliary dyskinesia: not too few, but not too many! Pediatr Pulmonol 2012; 47: 733-735.
7. Boon M, Vermeulen FL, Gysemans W, Proesmans M, Jorissen M, De Boeck K. Lung structure-function correlation in patients with primary ciliary dyskinesia. Thorax 2015; 70: 339-345.
8. Miller MR, Hankinson J, Brusasco V, Burgos F, Casaburi R, Coates A, Crapo R, Enright P, van der Grinten CP, Gustafsson P, Jensen R, Johnson DC, MacIntyre N, McKay R, Navajas D, Pedersen OF, Pellegrino R, Viegi G, Wanger J. Standardisation of spirometry. Eur Respir J 2005; 26: 319-338.
9. Nyilas S, Schlegtendal A, Singer F, Goutaki M, Kuehni CE, Casaulta C, Latzin P, Koerner-Rettberg C. Alternative inert gas washout outcomes in patients with primary ciliary dyskinesia. Eur Respir J 2017; 49.
10. Ramsey KA, Rosenow T, Turkovic L, Skoric B, Banton G, Adams AM, Simpson SJ, Murray C, Ranganathan SC, Stick SM, Hall GL. Lung Clearance Index and Structural Lung Disease on Computed Tomography in Early Cystic Fibrosis. Am J Respir Crit Care Med 2016; 193: 60-67.
11. Irving SJ, Ives A, Davies G, Donovan J, Edey AJ, Gill SS, Nair A, Saunders C, Wijesekera NT, Alton EW, Hansell D, Hogg C, Davies JC, Bush A. Lung clearance index and high-resolution computed tomography scores in primary ciliary dyskinesia. Am J Respir Crit Care Med 2013; 188: 545-549.
12. Santamaria F, Montella S, Tiddens H, Guidi G, Casotti V, Maglione M, de Jong PA. Structural and functional lung disease in primary ciliary dyskinesia. Chest 2008; 134: 351-357.

13. Pearce MS, Salotti JA, Little MP, McHugh K, Lee C, Kim KP, Howe NL, Ronckers CM, Rajaraman P, Sir Craft AW, Parker L, Berrington de Gonzalez A. Radiation exposure from CT scans in childhood and subsequent risk of leukaemia and brain tumours: a retrospective cohort study. Lancet 2012; 380: 499-505.
14. Puderbach M, Eichinger M, Gahr J, Ley S, Tuengerthal S, Schmahl A, Fink C, Plathow C, Wiebel M, Muller FM, Kauczor HU. Proton MRI appearance of cystic fibrosis: comparison to CT. Eur Radiol 2007; 17: 716-724.
15. Nyilas S, Bauman G, Sommer G, Stranzinger E, Pusterla O, Frey U, Korten I, Singer F, Casaulta C, Bieri O, Latzin P. Novel magnetic resonance technique for functional imaging of cystic fibrosis lung disease. Eur Respir J 2017; 50.
16. Thomen RP, Walkup LL, Roach DJ, Cleveland ZI, Clancy JP, Woods JC. Hyperpolarized 129Xe for investigation of mild cystic fibrosis lung disease in pediatric patients. J Cyst Fibros 2016.
17. Walkup LL, Thomen RP, Akinyi TG, Watters E, Ruppert K, Clancy JP, Woods JC, Cleveland ZI. Feasibility, tolerability and safety of pediatric hyperpolarized 129Xe magnetic resonance imaging in healthy volunteers and children with cystic fibrosis. Pediatr Radiol 2016; 46: 1651-1662.
18. Wielputz MO, Puderbach M, Kopp-Schneider A, Stahl M, Fritzsching E, Sommerburg O, Ley S, Sumkauskaite M, Biederer J, Kauczor HU, Eichinger M, Mall MA. Magnetic resonance imaging detects changes in structure and perfusion, and response to therapy in early cystic fibrosis lung disease. Am J Respir Crit Care Med 2014; 189: 956-965.
19. Costello JR, Kalb B, Martin DR. Incidence and Risk Factors for Gadolinium-Based Contrast Agent Immediate Reactions. Top Magn Reson Imaging 2016; 25: 257-263.
20. Smith LJ, West N, Hughes D, Marshall H, Johns CS, Stewart NJ, Chan HF, Rao M, Capener DJ, Bray J, Collier GJ, Hughes PJ, Norquay G, Schofield L, Chetcuti P, Moya E, Wild JM. Imaging Lung Function Abnormalities in Primary Ciliary Dyskinesia Using Hyperpolarised Gas Ventilation MRI. Ann Am Thorac Soc 2018.
21. Bauman G, Bieri O. Matrix pencil decomposition of time-resolved proton MRI for robust and improved assessment of pulmonary ventilation and perfusion. Magn Reson Med 2017; 77: 336-342.
22. Bauman G NS, Pusterla O, Heyer CM, Koerner-Rettberg C, Latzin P, Bieri O. . Pulmonary Fourier decomposition MRI compared to multiple breath washout and spirometry: A preliminary study in Primary Ciliary Dyskinesia. Proceedings of the 24th annual meeting of the ISMRM, Singapore 2016:2924 2016.
23. Neesen J, Kirschner R, Ochs M, Schmiedl A, Habermann B, Mueller C, Holstein AF, Nuesslein T, Adham I, Engel W. Disruption of an inner arm dynein heavy chain gene results in asthenozoospermia and reduced ciliary beat frequency. Hum Mol Genet 2001; 10: 1117-1128.
24. Cruz-Izquierdo S, Avila CM, Satovic Z, Palomino C, Gutierrez N, Ellwood SR, Phan HT, Cubero JI, Torres AM. Comparative genomics to bridge Vicia faba with model and closely-related

ANNALSATS Articles in Press. Published on 05-October-2018 as 10.1513/AnnalsATS.201712-967OC

legume species: stability of QTLs for flowering and yield-related traits. Theor Appl Genet 2012; 125: 1767-1782.

25. Fuchs HJ, Borowitz DS, Christiansen DH, Morris EM, Nash ML, Ramsey BW, Rosenstein BJ, Smith AL, Wohl ME. Effect of aerosolized recombinant human DNase on exacerbations of respiratory symptoms and on pulmonary function in patients with cystic fibrosis. The Pulmozyme Study Group. N Engl J Med 1994; 331: 637-642.
26. Eichinger M, Optazaite DE, Kopp-Schneider A, Hintze C, Biederer J, Niemann A, Mall MA, Wielputz MO, Kauczor HU, Puderbach M. Morphologic and functional scoring of cystic fibrosis lung disease using MRI. Eur J Radiol 2012; 81: 1321-1329.
27. Bauman G, Lutzen U, Ullrich M, Gaass T, Dinkel J, Elke G, Meybohm P, Frerichs I, Hoffmann B, Borggrefe J, Knuth HC, Schupp J, Prum H, Eichinger M, Puderbach M, Biederer J, Hintze C. Pulmonary functional imaging: qualitative comparison of Fourier decomposition MR imaging with SPECT/CT in porcine lung. Radiology 2011; 260: 551-559.
28. Bauman G, Puderbach M, Deimling M, Jellus V, Chefd'hotel C, Dinkel J, Hintze C, Kauczor HU, Schad LR. Non-contrast-enhanced perfusion and ventilation assessment of the human lung by means of fourier decomposition in proton MRI. Magn Reson Med 2009; 62: 656-664.
29. Bauman G, Puderbach M, Heimann T, Kopp-Schneider A, Fritzsching E, Mall MA, Eichinger M. Validation of Fourier decomposition MRI with dynamic contrast-enhanced MRI using visual and automated scoring of pulmonary perfusion in young cystic fibrosis patients. Eur J Radiol 2013; 82: 2371-2377.
30. Bauman G, Pusterla O, Bieri O. Ultra-fast Steady-State Free Precession Pulse Sequence for Fourier Decomposition Pulmonary MRI. Magn Reson Med 2016; 75: 1647-1653.
31. Stanojevic S, Wade A, Cole TJ, Lum S, Custovic A, Silverman M, Hall GL, Welsh L, Kirkby J, Nystad W, Badier M, Davis S, Turner S, Piccioni P, Vilozni D, Eigen H, Vlachos-Mayer H, Zheng J, Tomalak W, Jones M, Hankinson JL, Stocks J. Spirometry centile charts for young Caucasian children: the Asthma UK Collaborative Initiative. Am J Respir Crit Care Med 2009; 180: 547-552.
32. Singer F, Houltz B, Latzin P, Robinson P, Gustafsson P. A realistic validation study of a new nitrogen multiple-breath washout system. PLoS One 2012; 7: e36083.
33. Robinson PD, Latzin P, Verbanck S, Hall GL, Horsley A, Gappa M, Thamrin C, Arets HG, Aurora P, Fuchs SI, King GG, Lum S, Macleod K, Paiva M, Pillow JJ, Ranganathan S, Ratjen F, Singer F, Sonnappa S, Stocks J, Subbarao P, Thompson BR, Gustafsson PM. Consensus statement for inert gas washout measurement using multiple- and single- breath tests. Eur Respir J 2013; 41: 507-522.
34. Yammine S, Singer F, Gustafsson P, Latzin P. Impact of different breathing protocols on multiple-breath washout outcomes in children. J Cyst Fibros 2014; 13: 190-197.
35. Culver BH, Graham BL, Coates AL, Wanger J, Berry CE, Clarke PK, Hallstrand TS, Hankinson JL, Kaminsky DA, MacIntyre NR, McCormack MC, Rosenfeld M, Stanojevic S, Weiner DJ,

Laboratories ATSCoPSfPF. Recommendations for a Standardized Pulmonary Function Report. An Official American Thoracic Society Technical Statement. Am J Respir Crit Care Med 2017; 196: 1463-1472.

36. Brody AS, Klein JS, Molina PL, Quan J, Bean JA, Wilmott RW. High-resolution computed tomography in young patients with cystic fibrosis: distribution of abnormalities and correlation with pulmonary function tests. The Journal of pediatrics 2004; 145: 32-38.
37. J. C. Statistical power analysis for the behavioral sciences. 2nd Edn. London, Routledge. 1988.
38. Stahl M, Wielputz MO, Graeber SY, Joachim C, Sommerburg O, Kauczor HU, Puderbach M, Eichinger M, Mall MA. Comparison of Lung Clearance Index and Magnetic Resonance Imaging for Assessment of Lung Disease in Children with Cystic Fibrosis. Am J Respir Crit Care Med 2017; 195: 349-359.
39. Montella S, Maglione M, Bruzzese D, Mollica C, Pignata C, Aloj G, Manna A, Esposito A, Mirra V, Santamaria F. Magnetic resonance imaging is an accurate and reliable method to evaluate non-cystic fibrosis paediatric lung disease. Respirology 2012; 17: 87-91.
40. Dettmer S, Ringshausen F, Vogel-Claussen J, Fuge J, Faschkami A, Shin HO, Schwerk N, Welte T, Wacker F, Rademacher J. Computed tomography in adult patients with primary ciliary dyskinesia: Typical imaging findings. PLoS One 2018; 13: e0191457.
41. Kennedy MP, Noone PG, Leigh MW, Zariwala MA, Minnix SL, Knowles MR, Molina PL. High-resolution CT of patients with primary ciliary dyskinesia. AJR Am J Roentgenol 2007; 188: 1232-1238.
42. Davis SD, Rosenfeld M, Lee HS, Ferkol TW, Sagel SD, Dell SD, Milla C, Pittman JE, Shapiro AJ, Sullivan KM, Nykamp KR, Krischer JP, Zariwala MA, Knowles MR, Leigh MW, and Genetic Disorders of Mucociliary Clearance C. Primary Ciliary Dyskinesia: Longitudinal Study of Lung Disease by Ultrastructure Defect and Genotype. Am J Respir Crit Care Med 2018.

ANNALSATS Articles in Press. Published on 05-October-2018 as 10.1513/AnnalsATS.201712-967OC

Figure Legends

Figure 1. Venn diagram of PCD phenotypes. Venn diagrams for PCD phenotypes are clustered accordingly. Colored circles represent the different imaging and lung function modalities. [Lung Clearance index (LCI) from the nitrogen multiple breath washout, yellow; Sub-score of bronchiectasis and bronchial wall thickening from structural MRI, red; Forced expiratory volume in 1 second (FEV_1) from spirometry, blue; relative perfusion impairment (R_Q) from functional MRI, green; abnormal values are given in percentage]. ULN/LLN are defined as: LCI≥1.64 z-scores, FEV_1≤-1.64 z-scores, Sub-score of structural MRI ≥ 2 points, and R_Q≥19.3%. Numbers listed where circles overlap are common abnormal values in the respective modalities. Numbers do not sum up to 100%, because the overlap between functional and structural MRI is not displayed in the graph. Study participants from Figure 2 and Table E4 are marked as P1-P4.

Figure 2. Individual phenotypes. Sample images from (a) morphological T2-weighted structural MRI and (b-c) functional matrix pencil decomposition MRI including: (b) fractional ventilation (FV) maps, (c) perfusion-weighted (Q) maps. Low intensity regions (black and blue) on FV and Q maps correspond to regions with reduced signal amplitudes at respiratory and cardiac frequencies indicating functional defects (d and e). High values of fractional ventilation or perfusion are represented by yellow and red on the functional maps. Patient 1: Atelectasis of middle lobe and lingula with associated defects in Q and delay in blood arrival time (BAT). Moderate bronchial wall thickening and bronchiectasis in the lower lobes. FV defects are larger and in slightly different location (upper lobes) than expected from morphology. Age: 13 years;

nNo: 106,6 nl/min; TEM: IDA defect; Genetics: homozyg. DNAI1 mut. c.1232A>C. Patient 2: situs inversus, emphysematous changes of the apical parts of both lungs with associated decrease in Q. Mild to moderate bronchial wall thickening in both lower lobes with decreased homogeneity of Q and decrease in FV. Age: 28 years; nNo: 33 nl/min; TEM: not available; Genetics: not available. Patient 3: situs inversus, extensive bronchial wall thickening, bronchiectasis and mucus plugging in right lower lobe, lingula and middle lobe associated with defects in Q and FV and delayed BAT. Moderate changes of the left lower lobe. Minor changes of the upper lobes. Age: 22 years; nNo: 6.2 nl/min; TEM: ODA defect+tubul. disorg.; Genetics: homozyg. DNAH5 mut. ex.55 c.9346C>T. Patient 4: moderate bronchial wall thickening, bronchiectasis and mucus plugging with predominance in the lower lobes. Matched Q and FV abnormalities. Age: 8 years; nNo: 49.8 nl/min; TEM: IDA/ODA defect; Genetics: not available.

Figure 3. Lung clearance index (LCI) and structural MRI scores. Study participants with PCD were additionally divided in two groups by the sub-score mucus plugging: hollow circles indicate those study participants without relevant mucus plugging (<2 points in the sub-score mucus plugging) and closed circles indicate those study participants with relevant mucus plugging (≥2 points in the sub-score mucus plugging).

Figure 4. Lung clearance index (LCI) and functional MRI indices. A: Lung clearance index (LCI) and ventilation (R_{FV}) impairment of the lung as percentage. B: Lung clearance index (LCI) and perfusion (R_Q) impairment of the lung as percentage.

ANNALSATS Articles in Press. Published on 05-October-2018 as 10.1513/AnnalsATS.201712-967OC

Table 1 Clinical characteristics of study participants with PCD (N=30)

General characteristics	
Age at diagnosis (yr.; median (IQR))	4.2 (0.9 to 8.5)
Age at study enrollment (yr.; median (IQR))	13.4 (10.4 to 17.1)
Sex, n (males/females)	14/16
Height, cm	152.2 (138.5 to 167.3)
Weight, kg	49.8 (37.2 to 63.5)
Situs inversus	14 (47%)
[a]Diagnostics	
High-frequency-video microscopy (HVM) available	29 (97%)
Immotile	16 (55%)
Dyskinetic	13 (45%)
other	0
Transmission electron microscopy (TEM) available	24
ultrastructural abnormality	16 (66,7%)
inconclusive	2 (8,3%)
normal	6 (25%)
Not available	6 (20%)
Nasal nitric oxide (nNO) measurement done	30 (100%)
nNO median (min - max) in nl/min	18,7 (2,7 – 303,3)
subjects with low level <77 nl/min	26 (87%)
subjects with normal level >77nl/min	4 (13%)
Immunofluorescence (IF) with PCD defect identified	16
Genetic analysis with PCD defect identified	18

[a] For further diagnostic details see online supplement (Table E1)

Table 2 Functional and morphological MRI outcomes from study participants with PCD

Eichinger score (morphological MRI)			
	Median (IQR)	**Range**	*** Prevalence of abnormal values**
Total score (60 points)			
Score	10.3 (7 to 19)	3 to 28	
Bronchiectasis/ bronchial wall thickening/ (12 points)			
Sub-score	6 (4.5 to 8)	1.5 to 10.5	29/30 (97%)
Mucus plugging (12 points)			
Sub-score	2.3 (1 to 4)	0.5 to 8.5	18/30 (60%)
Consolidation (12 points)			
Sub-score	1.5 (0 to 3)	0 to 4.5	14/30 (47%)
Abscess/Sacculation (12 points)			
Sub-score	0 (0 to 0)	0.5 to 1	0/30 (0%)
Special findings (12 points)			
Sub-score	0 (0 to 0.5)	0 to 4.5	2/30 (7%)
Functional MRI (MP-MRI)			
Ventilation defect			
$R_{FV\ (\%)}$	24.2 (21.1 to 25.2)	16.7 to 28.7	14/27 (52%)
Perfusion defect			
$R_{Q\ (\%)}$	21.1 (19.4 to 25.9)	13.8 to 28.4	21/27 (78%)

All results are expressed as median (IQR), range, and percentage. A dedicated MRI score (*Eichinger score*) was used for morphological scoring. We used the mean of the morphological scores from two readers. The functional MRI (MP-MRI) gives results of the impairment of perfusion (R_Q) and ventilation (R_{FV}) in percentage of the lung volume. *The upper limit of normality was defined as ≥ 2 points for the sub-scores; for functional MRI indices ULN was used from published values (15).

ANNALSATS Articles in Press. Published on 05-October-2018 as 10.1513/AnnalsATS.201712-967OC

Table 3 Lung function outcomes in study participants with PCD

	Median (IQR)	**Range**	*** Prevalence of abnormal values**
N_2-MBW			
LCI [lung turnover]	10.8 (8.2 to 13.0)	6.6 to 17.9	
LCI [z-score]	8.3 (2.6 to 13.2)	-0.9 to 24	25/30 (83%)
S_{cond}	0.05 (0.03 to 0.07)	0 to 0.1	
S_{cond} [z-score]	2.8 (0.9 to 4.4)	-1.6 to 5.9	19/30 (63%)
S_{acin}	0.11 (0.08 to 0.26)	0.03 to 0.38	
S_{acin} [z-score]	1.7 (0.4 to 6.7)	-1.0 to 11.0	15/30 (50%)
Spirometry			
FEV_1 % pred.	99.1 (83.5 to 106.8)	28.9 to 113.6	
FEV_1 [z-score]	-0.5 (-1.6 to 0.3)	-5.7 to 0.77	8 (27%)

All results are expressed as median (IQR), range, and percentage. Outcome parameters from lung function measurements: lung clearance index (LCI); S_{cond} and S_{acin}, normalized phase III slope indices (see methods for explanation) and forced expiratory volume in 1 second (FEV_1). *ULN/LLN is defined as ± 1.64 z-score.

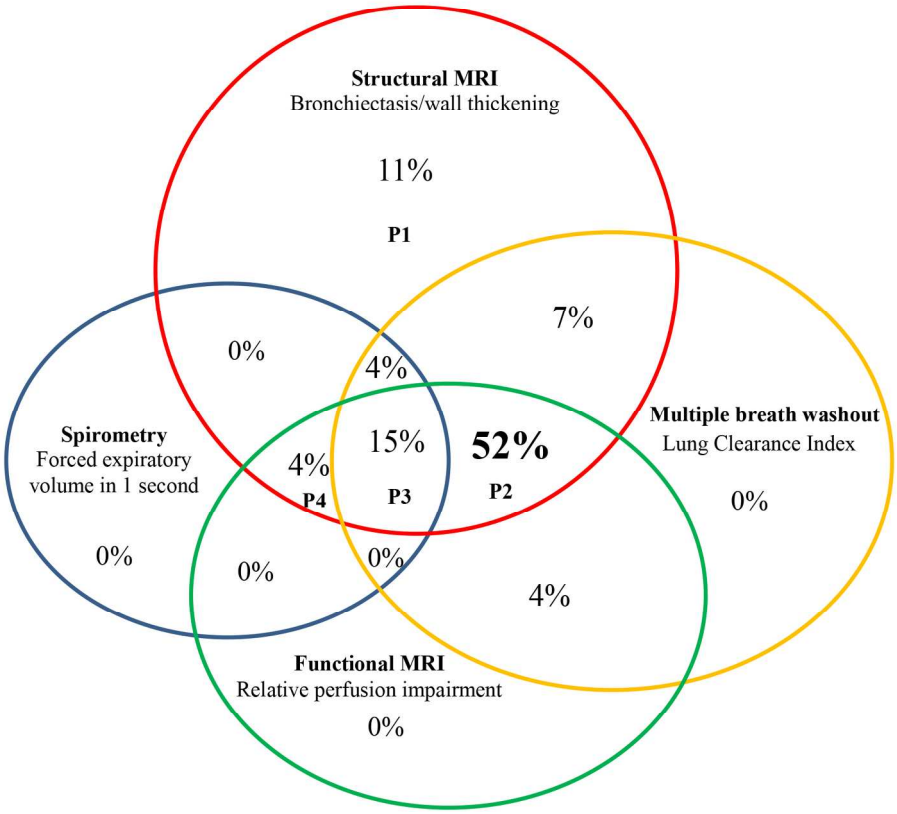

Venn diagrams for PCD phenotypes are clustered accordingly. Colored circles represent the different imaging and lung function modalities. [Lung Clearance index (LCI) from the nitrogen multiple breath washout, yellow; Sub-score of bronchiectasis and bronchial wall thickening from structural MRI, red; Forced expiratory volume in 1 second (FEV1) from spirometry, blue; relative perfusion impairment (RQ) from functional MRI, green; abnormal values are given in percentage]. ULN/LLN are defined as: LCI≥1.64 z-scores, FEV1≤-1.64 z-scores, Sub-score of structural MRI ≥ 2 points, and RQ≥19.3%. Numbers listed where circles overlap are common abnormal values in the respective modalities. Numbers do not sum up to 100%, because the overlap between functional and structural MRI is not displayed in the graph. Study participants from Figure 2 and Table E4 are marked as P1-P4.

178x178mm (300 x 300 DPI)

ANNALSATS Articles in Press. Published on 05-October-2018 as 10.1513/AnnalsATS.201712-967OC

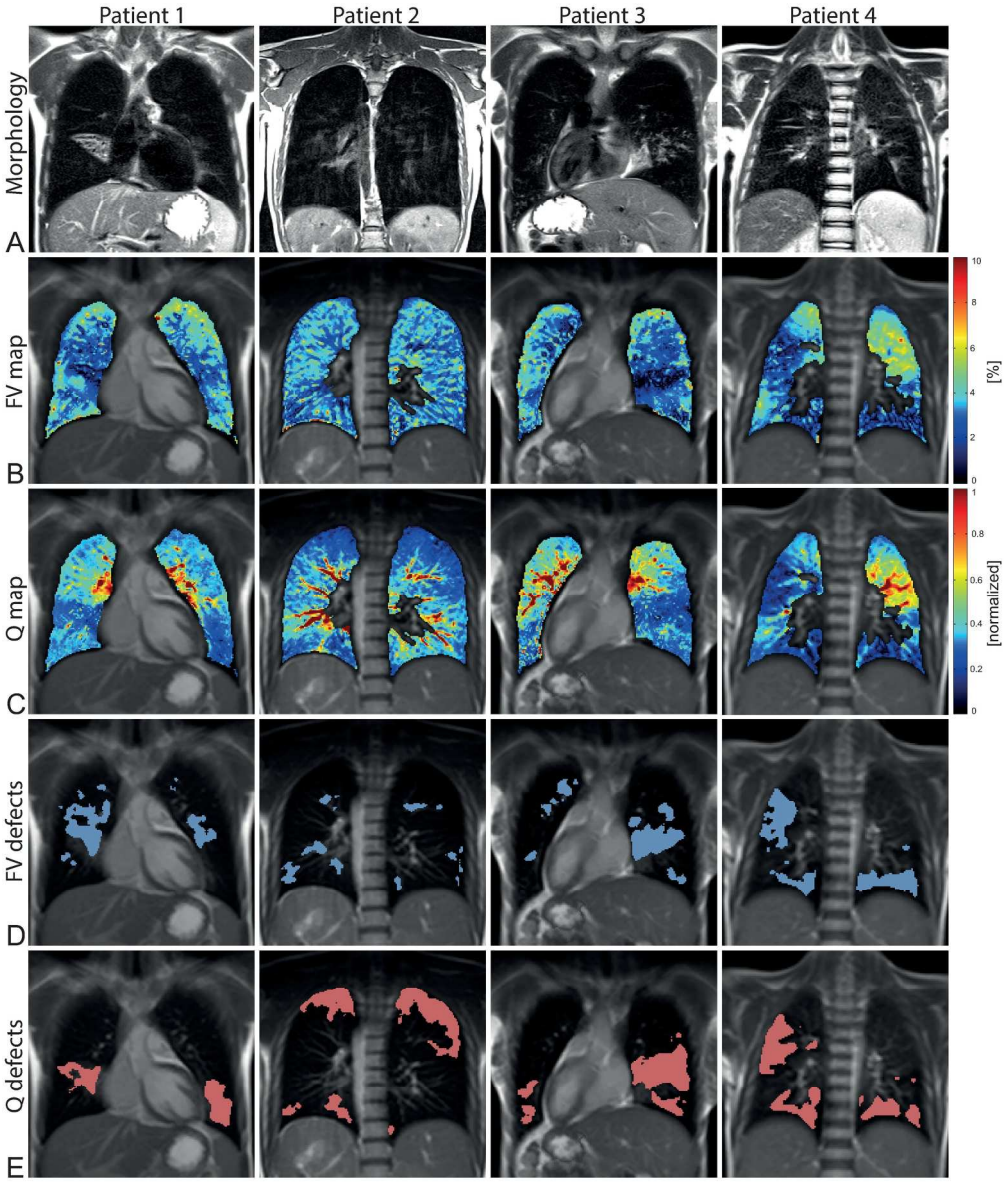

Sample images from (a) morphological T2-weighted structural MRI and (b-c) functional matrix pencil decomposition MRI including: (b) fractional ventilation (FV) maps, (c) perfusion-weighted (Q) maps. Low intensity regions (black and blue) on FV and Q maps correspond to regions with reduced signal amplitudes at respiratory and cardiac frequencies indicating functional defects (d and e). High values of fractional ventilation or perfusion are represented by yellow and red on the functional maps.
Patient 1: Atelectasis of middle lobe and lingula with associated defects in Q and delay in blood arrival time (BAT). Moderate bronchial wall thickening and bronchiectasis in the lower lobes. FV defects are larger and in slightly different location (upper lobes) than expected from morphology. Age: 13 years; nNo: 106,6 nl/min; TEM: IDA defect; Genetics: homozyg. DNAI1 mut. c.1232A>C.
Patient 2: situs inversus, emphysematous changes of the apical parts of both lungs with associated decrease in Q. Mild to moderate bronchial wall thickening in both lower lobes with decreased homogeneity of Q and decrease in FV. Age: 28 years; nNo: 33 nl/min; TEM: not available; Genetics: not available.
Patient 3: situs inversus, extensive bronchial wall thickening, bronchiectasis and mucus plugging in right lower lobe, lingula and middle lobe associated with defects in Q and FV and delayed BAT. Moderate changes

of the left lower lobe. Minor changes of the upper lobes. Age: 22 years; nNo: 6.2 nl/min; TEM: ODA defect+tubul. disorg.; Genetics: homozyg. DNAH5 mut. ex.55 c.9346C>T.
Patient 4: moderate bronchial wall thickening, bronchiectasis and mucus plugging with predominance in the lower lobes. Matched Q and FV abnormalities. Age: 8 years; nNo: 49.8 nl/min; TEM: IDA/ODA defect; Genetics: not available.

209x247mm (300 x 300 DPI)

ANNALSATS Articles in Press. Published on 05-October-2018 as 10.1513/AnnalsATS.201712-967OC

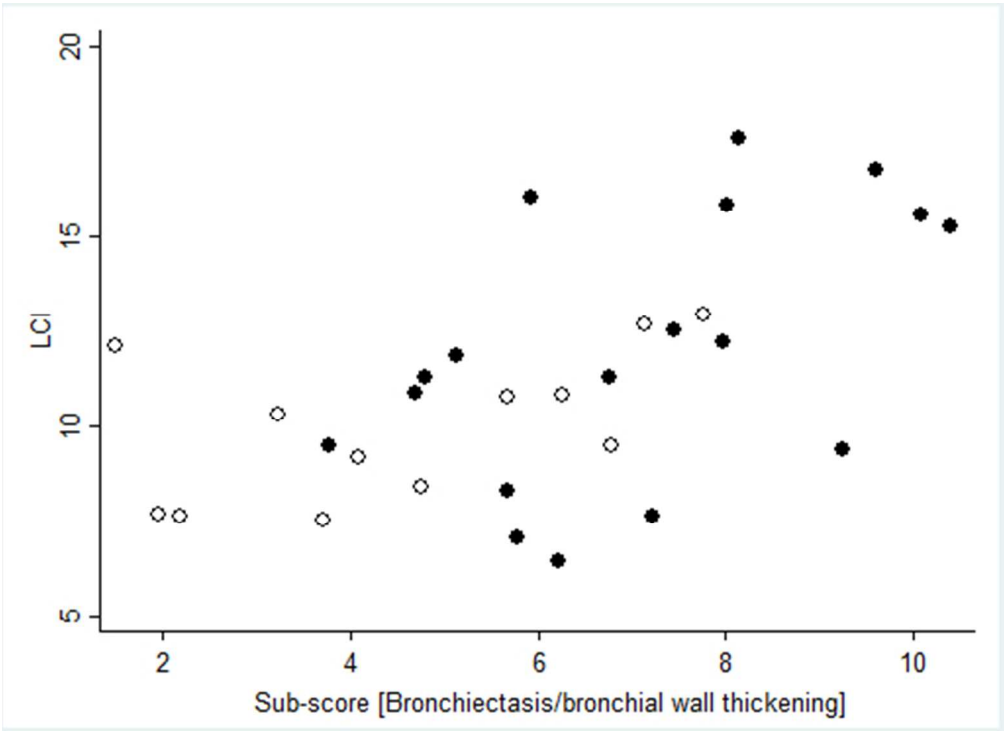

Study participants with PCD were additionally divided in two groups by the sub-score mucus plugging: hollow circles indicate those study participants without relevant mucus plugging (<2 points in the sub-score mucus plugging) and closed circles indicate those study participants with relevant mucus plugging (≥2 points in the sub-score mucus plugging).

180x130mm (72 x 72 DPI)

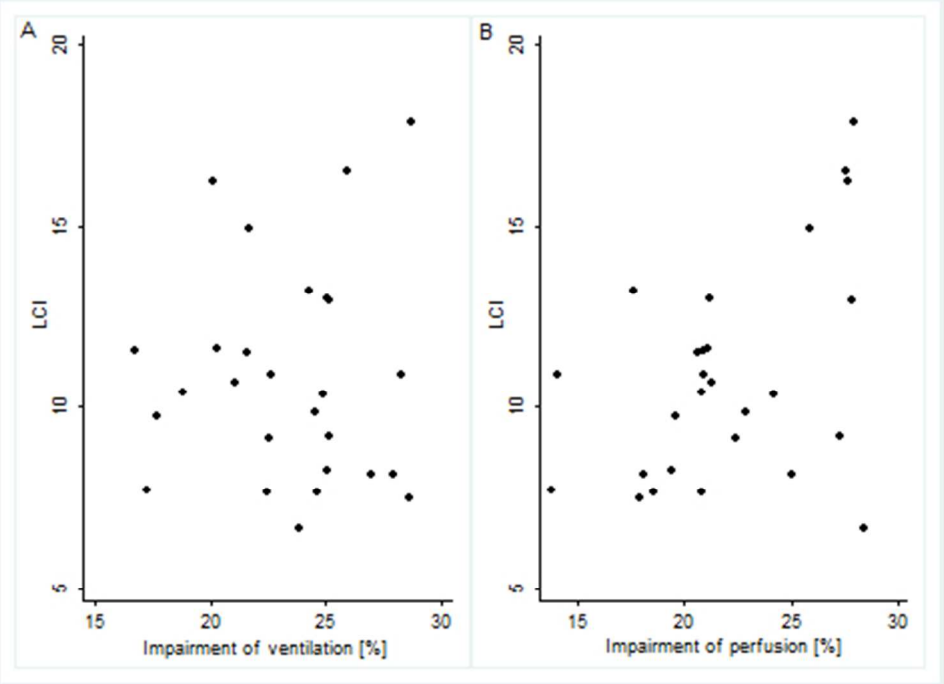

A: Lung clearance index (LCI) and ventilation (RFV) impairment of the lung as percentage.
B: Lung clearance index (LCI) and perfusion (RQ) impairment of the lung as percentage.

166x121mm (72 x 72 DPI)

ANNALSATS Articles in Press. Published on 05-October-2018 as 10.1513/AnnalsATS.201712-967OC

Structural and functional lung impairment in PCD:

Assessment with MRI and multiple breath washout in comparison to spirometry

Sylvia Nyilas; Grzegorz Bauman; Orso Pusterla; Gregor Sommer; Florian Singer; Enno Stranzinger; Christoph Heyer; Kathryn Ramsey; Anne Schlegtendal; Stefanie Benzrath; Carmen Casaulta; Myrofora Goutaki; Claudia E. Kuehni; Oliver Bieri; Cordula Koerner-Rettberg; Philipp Latzin

Online Data Supplement

Methods

Morphological MRI

The readers were blinded to the patients' clinical symptoms and history. Diagnostic quality of each image data set was rated on a 4-point Likert scale with 0 indicating the lowest (poor) and 3 the highest (excellent) image quality. The morphological MRI datasets were read by two board-certified, fellowship-trained radiologists with 9 and 14 years of experience in cross-sectional imaging of the chest. In brief, the Eichinger Score divided each lung into 6 lobes (with the lingula considered as a separate lobe) and scored for the presence of bronchiectasis/ bronchial wall thinkening in a central and peripheral zone. Central zone bronchiectasis/bronchial wall thickening: luminal diameter > corresponding artery; peripheral zone: visibility of bronchi within 1 cm of the pleural surface. Mucus plugging: area with a diameter greater than 0.3 cm. Abscess/sacculations: air filled or air fluid level within a minimum diameter of 1.5 cm. Consolidation: parenchym signal of the lung >2 cm, Special findings pleural effusion or reaction(1). The radiologist scores each disease parameter (bronchiectasis, mucus plugging, abscess and consolidation) separately in the lung as follows: 0 = not present; 1 = present, affecting ≤ 50% of the lobe; 2 = present, affecting > 50% of the lobe. The lobe scores for each component were summed to produce a score out of 12. The total score was defined as the sum of all scores.

Functional MRI

MP MRI technique (2) allows for simultaneous assessment of regional pulmonary perfusion and fractional ventilation without the need for the administration of an intravenous or inhaled contrast agents. Functional imaging was performed using time-resolved acquisitions with an ultra-fast steady-state free precession (ufSSFP) pulse sequence (3, 4). Multiple coronal slices were acquired in order to cover the whole lung volume. Neither ECG nor any respiratory

ANNALSATS Articles in Press. Published on 05-October-2018 as 10.1513/AnnalsATS.201712-967OC

triggering method is required during the scan. MP decomposition technique takes advantage from variations of regional MR signal intensity in the lung tissue caused by respiratory and cardiac cycles. In the inspiration the regional lung volume increases while the signal intensity decreases. The opposite takes place during expiration. Thus, the signal intensity in the lung is determined by the phase of the respiratory cycle and can be scaled linearly in the tidal volume breathing region. The signal intensity in the lung parenchyma is also modulated by the cardiac cycle. Fresh unsaturated blood entering the slice being imaged increases the regional signal intensity. Both physiological cycles correspond to different frequencies and can be spectrally retrieved in the time-resolved dataset. However, prior to further post-processing, the acquired datasets are subject to elastic image registration for the compensation of respiratory motion. Subsequently, pixel-wise spectral analysis is performed on the motion-corrected data using the MP decomposition to identify frequency components of the physiological cycles. Matrix pencil (MP) decomposition method was applied to generate maps of regional fractional ventilation, which reflects changes of lung parenchyma density during respiration, as well as relative perfusion maps. The signal distributions on the functional images in the segmented region of interests were analyzed to estimate threshold values indicating a functional impairment of 75% of the median value of the voxel distributions.

Results

Data Quality

Morphological MRI

The average diagnostic quality of the morphological MRI data sets was good (average score = 2.0) with 26 datasets rated excellent (score 3), 25 good (score 2) and 9 fair (score 1).

Functional MRI

Due to logistic reasons, no functional images were obtained in three patients. All MR images included into the analysis were of sufficient diagnostic quality.

ANNALSATS Articles in Press. Published on 05-October-2018 as 10.1513/AnnalsATS.201712-967OC

Legend to the figures

Figure E1

FEV_1 and structural MRI sub-scores for bronchiectasis/bronchial wall thickening. Patients with PCD were additionally divided in two groups by the sub-score mucus plugging: hollow circles indicate those patients without relevant mucus plugging (<2 points in the sub-score mucus plugging) and closed circles indicate those patients with relevant mucus plugging (≥2 points in the sub-score mucus plugging).

Figure E2

Relative perfusion impairment (R_Q) and structural MRI sub-scores for bronchiectasis/bronchial wall thickening. Patients with PCD were additionally divided in two groups by the sub-score mucus plugging: hollow circles indicate those patients without relevant mucus plugging (<2 points in the sub-score mucus plugging) and closed circles indicate those patients with relevant mucus plugging (≥2 points in the sub-score mucus plugging).

Figure E3

Lung clearance index (LCI) and structural MRI total scores

Table E1 Patients' diagnostic features including causative mutations

Patient	Situs	[a]nNO	[b]HFVM	[b]TEM	IF	Genetics	Comments
1	si	normal (251,7 nl/min)	3x mildly dyskinetic (uncoordinated beating pattern, winding movement)	1x normal, 1x reduced ODA/IDA	Lack of CCDC11 and DNALI1	homozygous loss of function CCDC11 mutation c.121C>T	bronchiectasis in right lower lobe, bronchial wall thickening in both lower lobes
2	si	normal (303,4 nl/min)	2x mildly dyskinetic (uncoordinated beating pattern, reduced amplitude)	2x missing of central pairs in 30% of cilia, 1x + ODA defect + reduced /IDA	Lack of DNAH5	homozygous loss of function CCDC11 mutation c.121C>T	bronchial wall thickening in middle lobe, elevated LCI
3	ss	low	2x immotile	ODA/IDA defect, + in 20% missing of central pairs	not done	homozygous DNAH5 mutation c.8757G>C, + two heterozygous mutations: in DNAI1 c.48+2dupT and in DNAAF3 c.296C>G	
4	ss	low	2x dyskinetic	IDA/ODA defect	DNAH5 and GAS8 present	awaiting results	
5	si	low	2x immotile with some fasciculation	normal	not done	awaiting results	one additional sibling affected (not included in the study), also situs inversus, low nNO
6	ss	low	immotile with some fasciculation	IDA/ODA defect	Lack of DNAH5	not done	
7	si	low	immotile with some fasciculation	IDA/ODA defect + tubulus dysorganizat.	DNAH5 staining abnormal	homozygous ARMC4 mutation c.2675C>A	
8	si	low	2x immotile	not done	not done	not done	typical PCD phenotype including neonatal distress, and middle lobe atelectasis
9	si	low	immotile with some fasciculation	IDA/ODA defect	Lack of DNAH5	2 DNAH5 mutations c.8029C>T and	

ANNALSATS Articles in Press. Published on 05-October-2018 as 10.1513/AnnalsATS.201712-967OC

						c.10615C>T	
10	si	low	immotile	normal	Lack of DNAH5	2 DNAH5 mutations c.13194_13197del and c.10615C>T	
11	si	low	immotile	ODA defect + tubulus dysorganizat.	not done	homozygous DNAH5 mutation ex.55 c.9346C>T	
12	ss	low	2x immotile	ODA defect + reduced IDAs	Lack of DNAH5	homozygous DNAH5 mutation c.2224C>T	
13	ss	low	2x dyskinetic	normal	DNAH5 limited to ciliary base	homozygous DNAI1 mutation c.48+2insT	
14	si	low	2x immotile with some fasciculation	not done	not done	awaiting results	neonat distress, middle lobe atelectasis, radioaerosole mucociliary clearance test pathological
15	ss	low	2x immotile with some fasciculation	2x IDA defect + tubulus dysorganizat.	not done	homozygous CCDC39 mutation c.610_613delTTAG	
16	ss	low	immotile	ODA defect	Lack of DNAH5	not done	
17	ss	normal (106,6 nl/min)	2x dyskinetic (uncoordinated and reduced frequency)	2x IDA defect	not known	homozygous DNAI1 mutation c.1232A>C	
18	si	low	2x immotile	result not known (done in native country)	Lack of DNAH5	SPAG1 heterozygous mutation p.Q672* and 11kb deletion	
19	si	low	too few ciliated cells	too few cilia	not done	homozygous nonsense DNAH5 mutation c.2224C>T for p.Arg742X	
20	ss	low	2x immotile	normal	Lack of DNAH5	2 DNAH5 mutations c.5710-2A>G and c.10815delT	
21	ss	low	2x immotile with some fasciculation	IDA/ODA defect	Lack of DNAH5	not done	
22	si	normal (84,8 nl/min)	very fast (>16Hz) beating, reduced amplitude + backwards movement	1x normal, 1x slightly reduced IDAs	DNAH5, GAS8 and RSPH9 normal	2 mutations in DNAH11 c.1710+1G>C and c.8920A>G	

23	ss	low	2x immotile	ODA defect	not done	homozygous DNAH5 mutation c.6057delT and heterozygous DNAH11 mutation c.9469C>T	Sibling of 24
24	si	low	2x immotile	ODA defect, IDAs slightly reduced	not done	homozygous DNAH5 mutation c.6057delT	Sibling of 23
25	si	low	dyskinetic (uncoordinated, reduced amplitude)	IDAs missing	Lack of DNAH5 and DNALI1	homozygous DYX1C1 mutation c.583delA	
26	ss	low	2x: dyskinetic (slow uncoordinated beating), same as sibling (patient 27)	not done	not done	not done	Sibling of 27
27	ss	low	2x: dyskinetic (slow uncoordinated beating), same as sibling (patient 26)	not done	not done	not done	Sibling of 26
28	ss	low	2x dyskinetic	normal	Lack of DNAH5	not done (lives abroad)	Sibling of 29, situs inversus in a third PCD-affected sibling (not in study as too young for lung function)
29	ss	low	2x dyskinetic	normal	Lack of DNAH5	not done (lives abroad)	Sibling of 28, situs inversus in a third PCD-affected sibling (not included in this study)
30	ss	low	2x dyskinetic	ODA defect	Lack of DNAH5	not done (lives abroad)	

[a] measurements done at least on 3 occasions, [b] "2x" etc. indicates the number of performed tests, si= situs inversus, ss= situs solitus.

ANNALSATS Articles in Press. Published on 05-October-2018 as 10.1513/AnnalsATS.201712-967OC

Table E2 Morphological MRI scoring from two readers

Eichinger score (morphological MRI)			
	Reader 1	Reader 2	ICC (95%CI)
Total score			
Score	11 (9 to 18)	8.5 (5 to 20)	0.67 (0.44 to 0.82)
Bronchiectasis/ bronchial wall thickening			
Subscore	7 (6 to 8)	5 (3 to 7)	0.51 (0.27 to 0.75)
Mucus plugging			
Subscore	3 (1 to 5)	2(1 to 4)	0.78 (0.60 to 0.89)
Consolidation			
Subscore	2 (0 to 3)	2 (0 to 3)	0.82 (0.67 to 0.91)
Abscess/Sacculation			
Subscore	0 (0 to 0)	0 (0 to 0)	
Special findings			
Subscore	0 (0 to 1)	0 (0 to 0)	0.43 (0.18 to 0.71)

All results are expressed as median (+ IQR) or as ICC (95% CI). A dedicated MRI score (Eichinger score) was used for morphological scoring. Reading was performed by two independent radiologists: Reader 1 and Reader 2. Interobserver agreement was calculated by using the intraclass correlation coefficient (ICC).

Table E3 Distribution of MRI structural anomalies in upper vs. middle vs. lower lobes

	Bronchiectasis/ bronchial wall thickening			Mucus plugging		
Score	**0**	**1**	**2**	**0**	**1**	**2**
Right lung						
Upper lobe	7 (23%)	22 (73%)	1 (3%)	28 (93%)	2 (7%)	-
Middle lobe	2 (7%)	12 (40%)	16 (53%)	11 (37%)	10 (33%)	9 (30%)
Lower lobe	-	17 (57%)	13 (43%)	11 (37%)	15 (50%)	4 (13%)
Left lung						
Upper lobe	5 (17%)	24 (80%)	1 (3%)	25 (83%)	5 (17%)	-
Lower lobe	2 (7%)	18 (60%)	10 (33%)	18 (60%)	9 (30%)	3 (10%)
Lingula	7 (23%)	14 (47%)	9 (30%)	19 (63%)	6 (20%)	5 (17%)

Bronchiectasis/bronchial wall thickening and mucus plugging with detailed count of patients with PCD N (%). Detailed scoring from Reader 1.

Table E4 Concordance between different modalities on an individual level in four study participants with PCD

	Patient 1	Patient 2	Patient 3	Patient 4

ANNALSATS Articles in Press. Published on 05-October-2018 as 10.1513/AnnalsATS.201712-967OC

Age, years	13	28	22	8
Gender	male	female	female	male
	Normal spirometry		**Abnormal spirometry**	
FEV_1 [%]	104	109	**84**	**83**
FEV_1 [z-score]	-0.08	0.36	**-1.64**	**-1.67**
FVC [z-score]	-0.83	1.41	-0.03	**-2.50**
Multiple breath washout				
LCI	7.6	10.3	17.9	6.6
LCI [z-score]	1.3	**7.3**	**24**	-0.9
Functional MRI				
R_{FV} [%]	22.4	**24.9**	**28.7**	23.9
R_Q [%]	18.6	**24.2**	**28.0**	**28.4**
Morphological MRI				
Main characteristics	**Atelectasis**	**Emphysematous**	**Bronchiectasis and mucus plugging**	**Mixed morphology**
Bronchial wall thickening and mucus plugging	Moderate	Mild to moderate	Extensive	Moderate
Atelectasis	Middle lobe (complete), Lingula (partial)			Left upper lobe (subsegmental)
Eichinger score	**24**	**5**	**26**	**10**
Situs type	normal	situs inversus	situs inversus	normal
Diagnostics				
nNO in nl/min	106.6	**33**	**6.2**	**49.8**
TEM	IDA defect	not available	ODA defect and tubul. disorg.	IDA/ODA defect
Genetic analysis	homozyg. DNAI1 mut. c.1232A>C.	not available	Homozygous DNAH5 mut. ex. 55 c. 9346C>T mutations	not available
Pathological values are marked in bold.				

Table E5 Correlation between lung function parameters with MRI-defined morphological and functional abnormalities in patients with PCD

		MRI-defined morphological indices					**Functional MRI indices**	
		Subscores					**Impairment of ventilation (R_{FV}) (r, p-value)**	**Impairment of perfusion (R_Q) (r, p-value)**
Indices	**Total score (r, p-value)**	**Bronchiectasis/ Bronchial wall thickening (r, p-value)**	**Mucus plugging (r, p-value)**	**Consolidation (r, p-value)**	**Abscess/Sacculation (r, p-value)**	**Special findings (r, p-value)**		
LCI	0.54, **0.002**	0.55, **0.002**	0.41, **0.026**	0.36, 0.050	0.04, 0.841	0.35, 0.057	-0.05, 0.793	0.34, 0.081
S_{cond}	0.18, 0.3506	0.22, 0.238	0.23, 0.222	0.29, 0.115	-0.22, 0.237	0.007, 0.972	-0.27, 0.167	0.26, 0.182
S_{acin}	0.28, 0.140	0.27, 0.152	0.32, 0.080	0.08, 0.656	0.41, **0.023**	0.28, 0.133	-0.18, 0.376	-0.01,0.947
FEV_1	-0.59, **<0.001**	-0.54, **0.002**	-0.61, **<0.001**	-0.46, 0.011	-0.32, 0.088	-0.45, **0.012**	0.13, 0.527	-0.37, 0.060

Significant correlations (Spearman correlation coefficients) are marked in bold. P-values < 0.05 were considered statistically significant. Correlation between dedicated morphology MRI score (mean from both readers) and ventilation (R_{FV}) , perfusion (R_Q) impairment of the lung from functional MRI (MP-MRI) with different lung function outcomes: lung clearance index (LCI); S_{cond}, and S_{acin}, normalized phase III slope indices (see methods for explanation) and forced expiratory volume in 1 second (FEV_1).

ANNALSATS Articles in Press. Published on 05-October-2018 as 10.1513/AnnalsATS.201712-967OC

References

1. Eichinger M, Optazaite DE, Kopp-Schneider A, Hintze C, Biederer J, Niemann A, Mall MA, Wielputz MO, Kauczor HU, Puderbach M. Morphologic and functional scoring of cystic fibrosis lung disease using MRI. Eur J Radiol 2012; 81: 1321-1329.
2. Bauman G, Bieri O. Matrix pencil decomposition of time-resolved proton MRI for robust and improved assessment of pulmonary ventilation and perfusion. Magn Reson Med 2017; 77: 336-342.
3. Bauman G, Pusterla O, Bieri O. Ultra-fast Steady-State Free Precession Pulse Sequence for Fourier Decomposition Pulmonary MRI. Magn Reson Med 2016; 75: 1647-1653.
4. Bieri O. Ultra-fast steady state free precession and its application to in vivo H morphological and functional lung imaging at 1.5 tesla. Magn Reson Med 2013.

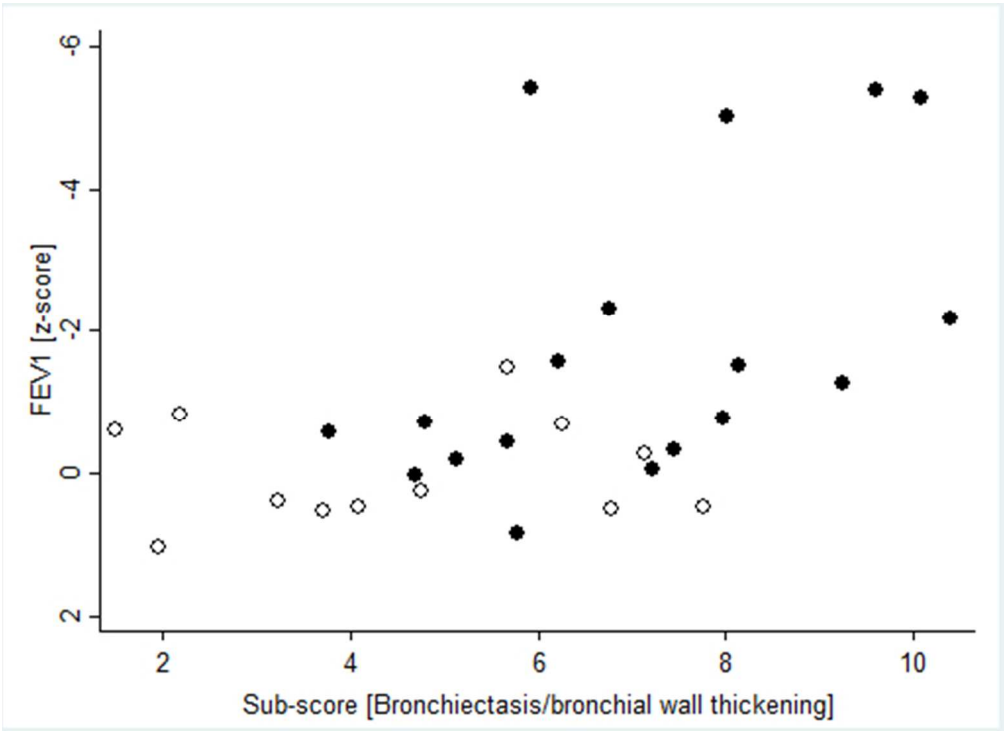

FEV1 and structural MRI sub-scores for bronchiectasis/bronchial wall thickening. Patients with PCD were additionally divided in two groups by the sub-score mucus plugging: hollow circles indicate those patients without relevant mucus plugging (<2 points in the sub-score mucus plugging) and closed circles indicate those patients with relevant mucus plugging (≥2 points in the sub-score mucus plugging).

180x130mm (72 x 72 DPI)

ANNALSATS Articles in Press. Published on 05-October-2018 as 10.1513/AnnalsATS.201712-967OC

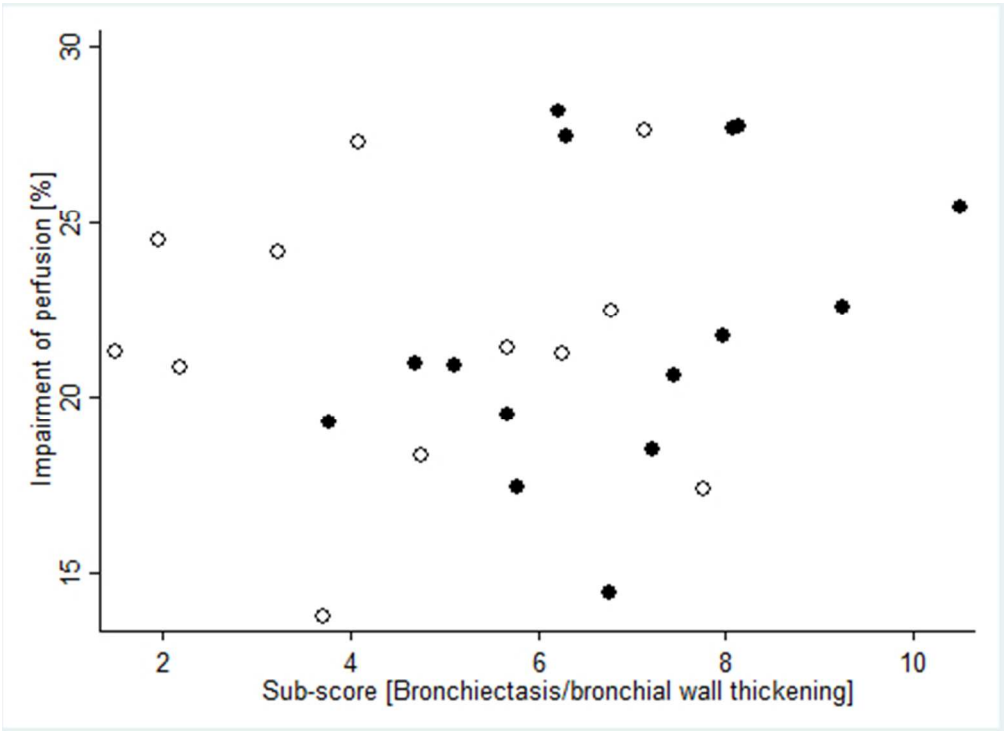

Relative perfusion impairment (RQ) and structural MRI sub-scores for bronchiectasis/bronchial wall thickening. Patients with PCD were additionally divided in two groups by the sub-score mucus plugging: hollow circles indicate those patients without relevant mucus plugging (<2 points in the sub-score mucus plugging) and closed circles indicate those patients with relevant mucus plugging (≥2 points in the sub-score mucus plugging).

180x130mm (72 x 72 DPI)

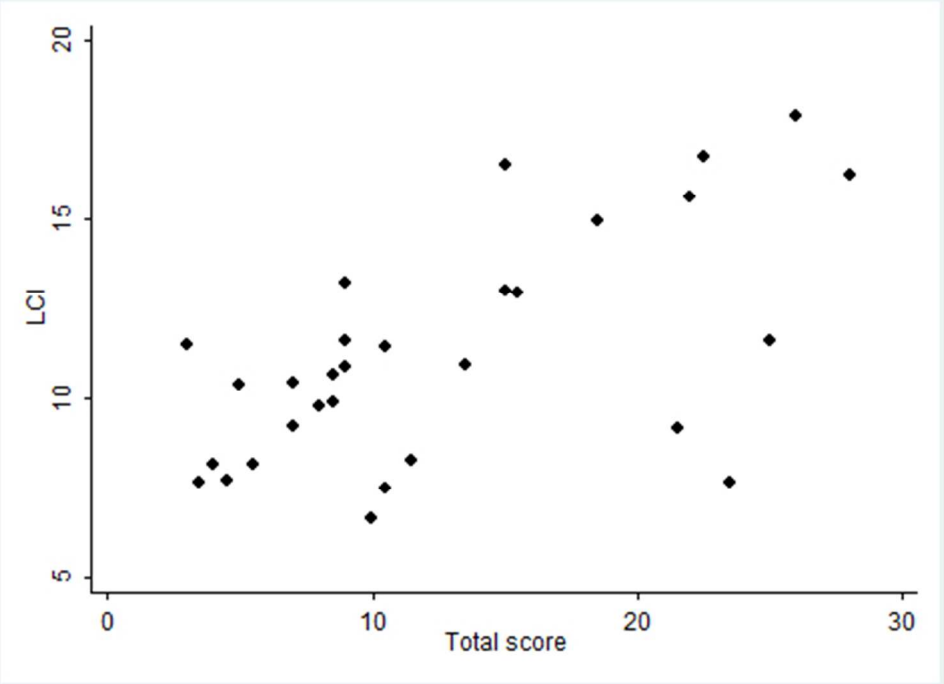

Lung clearance index (LCI) and structural MRI total scores

166x121mm (72 x 72 DPI)